Applied Clay Science 112–113 (2015) 62–67

Contents lists available at ScienceDirect

Applied Clay Science

journal homepage: www.elsevier.com/locate/clay

Research paper

Thermal analysis evidence for the location of zwitterionic surfactant on clay minerals

Lingya Ma [a,b,c], Jianxi Zhu [a,c], Hongping He [a,c,*], Yunfei Xi [d], Runliang Zhu [a,c], Qi Tao [a,c], Dong Liu [a,c]

[a] CAS Key Laboratory of Mineralogy and Metallogeny, Guangzhou Institute of Geochemistry, Chinese Academy of Sciences, Guangzhou 510640, China
[b] University of Chinese Academy of Sciences, Beijing 100049, China
[c] Guangdong Provincial Key Laboratory of Mineral Physics and Material, Guangzhou 510640, China
[d] Nanotechnology and Molecular Science Discipline, Faculty of Science and Engineering, Queensland University of Technology, 2 George Street, GPO Box 2434, Brisbane, QLD 4000, Australia

ARTICLE INFO

Article history:
Received 18 March 2015
Received in revised form 27 April 2015
Accepted 28 April 2015
Available online 25 May 2015

Keywords:
Zwitterionic surfactant
Organoclays
Pillared interlayered clay
Thermal decomposition
Talc
Montmorillonite

ABSTRACT

The exact location of surfactant molecules on clay minerals is critical for the synthesis of clay polymer nanocomposites and their applications in environmental remediation. The location and thermal characteristics of zwitterionic surfactant (Z16) composites with montmorillonite (Mt), Al_{13}-pillared montmorillonite (AlPMt), calcined AlPMt (AlPMt/500), and talc (Tlc) were investigated by using X-ray diffraction (XRD) and thermogravimetric analysis (TG). The basal spacing of Mt was markedly increased after modification with Z16, while that of Tlc, AlPMt, and AlPMt/500 was essentially unchanged. The decomposition temperature of Z16/Tlc composite (~294 °C) was similar to that of the pure surfactant. Sulfobetaine apparently failed to penetrate into the interlayer space of talc; instead it was confined to external surfaces. On the other hand, the DTG pattern of Z16-modified Mt showed two main peaks (404 and 336 °C), indicating two different intercalation mechanisms of Z16 on Mt. Sulfobetaine, loaded to AlPMt and AlPMt/500, was found to decompose at 355 and 370 °C, respectively, suggesting that Z16 occupied the interpillar space in these samples. Much more Z16 was taken up by AlPMt than by AlPMt/500, although the specific surface areas of both materials were practically identical, suggesting that the surfactant molecules in the interlayer space of AlPMt were largely adsorbed by electrostatic attraction between the negatively charged groups of Z16 and the positively charged Al_{13} cations.

1. Introduction

Clay minerals are important raw materials of choice for the novel materials because they are abundant, inexpensive and environmentally friendly (Bergaya and Lagaly, 2013). Being hydrophilic, however, many representative species, such as montmorillonite and saponite, as well as their inorganic pillared forms are immiscible in organic media, limiting their scope for industrial and environmental applications. Surface modification through intercalation and grafting of organic species is, therefore, an important step in processing clay minerals for industrial applications (Bergaya and Lagaly, 2001; Bergaya et al., 2011; He et al., 2013, 2014). In particular, surfactant-modified montmorillonites ('organoclay') have received a great deal of attention because of their great performance in environmental protection, remediation (Zhu and Chen, 2000; Zhu et al., 2000; Theng et al., 2008) and the synthesis of clay polymer nanocomposites (Ray and Okamoto, 2003; Theng, 2012). A recent development of great interest is the preparation of surfactant-modified pillared interlayered clays (PILC) (Tahani et al., 1999; Annabi-Bergaya, 2008; Zhu et al., 2009a; He et al., 2014; Ma et al., 2014a, 2014b). Having both hydrophilic and hydrophobic surface properties, these inorganic–organic clays (IOC) are potentially capable of synchronically removing organic and inorganic contaminants in wastewater (Zhu and Zhu, 2007; Bouberka et al., 2009; Zhu et al., 2009b; Ouellet-Plamondon et al., 2012).

Previous studies have shown that the type of organic surfactant used can markedly influence the structural characteristics and adsorptive behavior of organoclays (OC) (Dentel et al., 1998; Shen, 2002; Heinz et al., 2007; Chitrakar et al., 2011). In this respect, zwitterionic surfactants, such as sulfobetaine, might significantly improve the adsorption capacity of OC. Besides containing both positively charged (quaternary ammonium) and negatively charged (sulfonate) functional groups, sulfobetaine is highly water-soluble, biodegradable and non-toxic (Qi et al., 2008; Zhu et al., 2011).

The location and thermal behavior of surfactant molecules on external and interlayer surfaces of clay minerals have been the subject of many investigations (Xie et al., 2002; He et al., 2005; Xi et al., 2005, 2007; Kooli, 2009; Zhu et al., 2012; Ma et al., 2014a). Cationic surfactants may associate with montmorillonite surfaces as (a), intercalated cations; (b), intercalated molecules (ion pairs); and (c), molecules filling interparticle pores (He et al., 2005; Xi et al., 2005; Zhu et al., 2012). On heating, intercalated and pore-filling surfactant molecules

* Corresponding author at: Guangzhou Institute of Geochemistry, Chinese Academy of Sciences (CAS), Wushan, Guangzhou 510640, China. Tel.: +86 20 85290257; fax: +86 20 85290130.
E-mail address: hehp@gig.ac.cn (H. He).

http://dx.doi.org/10.1016/j.clay.2015.04.021
0169-1317/

commonly decompose at a lower temperature than that shown by their intercalated cationic counterparts (He et al., 2005; Xi et al., 2005; Zhu et al., 2012). The location of zwitterionic surfactant on clay minerals significantly affected the structure and application of obtained OMt. In previous studies (Zhu et al., 2012; Ma et al., 2014b), zwitterionic surfactants modified montmorillonites and PILC showed different structures with those modified by cationic surfactant. However, the location and behavior of zwitterionic surfactant on clay mineral surface has not yet been clarified, which is important to understand the modification mechanism.

Therefore, in this study, some evidences of the location of zwitterionic surfactant on clay mineral surfaces were tried to be found out by thermal analysis combined with X-ray diffraction (XRD), specific surface area (SSA) and pore size analysis. Zwitterionic surfactant — hexadecyldimethyl (3-sulfonatopropyl) ammonium (Z16) (Fig. 1) was selected as a surface-modifying agent for talc (Tlc), montmorillonite (Mt), Al_{13}-pillared Mt (AlPMt), and AlPMt after calcination at 500 °C (AlPMt/500). The decomposition temperature of the different samples could be directly obtained from analyzing the respective TG and derivative TG (DTG) curves (Frost et al., 2009; Liu et al., 2013). For all three Mt samples, the surfactant was capable of penetrating the interlayer space. For comparison, this study also assessed the thermal stability of Z16-modified talc where adsorption of surfactant was confined to external particle surfaces. The SSA of the clay samples was determined by adsorption of N_2 gas at −195.79 °C. The results suggest that adsorbed sulfobetaine may adopt a variety of conformations in the interlayer and external surfaces of clay minerals.

2. Materials and methods

2.1. Materials

Calcium montmorillonite (Mt), with a cation exchange capacity of 110.5 $cmol_{(+)}$/kg, was obtained from Inner Mongolia, China. The talc sample (Tlc) was obtained from Longsheng, Guangxi province, China. Sulfobetaine (Z16), with a chemical formula of $C_{21}H_{45}NO_3S$ and a purity of 99%, was supplied by Nanjing Robiot Co. Ltd., China. Analytical grade $AlCl_3 \cdot 6H_2O$ and Na_2CO_3 were supplied by Guangzhou Chemical Reagent Factory, China.

2.2. Synthesis of Al-pillared montmorillonite

A hydroxyl-aluminum solution, containing Al_{13} cations, was prepared by slowly adding a 0.5 M Na_2CO_3 solution to a 1.0 M solution of $AlCl_3$ at a rate of 1 mL/min with vigorous stirring in a water bath at 60 °C to give a final OH^-/Al^{3+} ratio of 2.4. The mixture was continuously stirred for 12 h, after which it was allowed to 'age' for 24 h at 60 °C. Montmorillonite was then added to the mixture to give an Al/clay ratio of 10 mmol/g. The dispersion was stirred for 24 h, and then aged for 24 h at 60 °C. The resultant AlPMt was collected by centrifugation, washed 8 times with distilled water, and then freeze-dried for 48 h. Its calcined derivative (AlPMt/500) was obtained by heating AlPMt in an oven at 500 °C for 8 h.

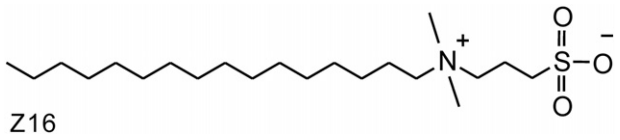

Fig. 1. Chemical structure of the zwitterionic surfactant, hexadecyldimethyl (3-sulfonatopropyl) ammonium, denoted as Z16.

2.3. Surfactant modification

Surfactant modification was carried out by adding 1 g of a given clay mineral sample to 20 mL of a 0.11 M solution of Z16 at 60 °C, and stirring for 12 h. The products were collected by centrifugation, washed 8 times with distilled water (except for the mixture of Tlc and Z16, which was washed only once) in order to remove Z16 molecules, associated with external particle surfaces, and then freeze-dried for 48 h. The various Z16-modified materials were denoted as Z16–Tlc, Z16–Mt, Z16–AlPMt, and Z16–AlPMt/500.

2.4. Characterization

Powder X-ray diffraction (XRD) patterns were recorded on a Bruker D8 Advance diffractometer with Ni-filtered CuKα radiation (λ = 0.154 nm, 40 kV and 40 mA) with 2.3° Soller slits, 1.0 mm divergence slit and 0.1 mm receiving slit. Patterns were collected between 1° and 80° (2θ) at a scanning speed of 2° (2θ) min^{-1} with a 0.01 2θ step size and a 0.3 s counting time. Samples used for XRD were random powder.

Thermogravimetric analysis (TG) was performed on a Netzsch STA 409PC instrument. The samples were heated from 30 to 1000 °C at a rate of 10 °C/min under a flow of high-purity nitrogen (60 mL/min). The differential thermogravimetric (DTG) curves were directly derived from the corresponding TG curves.

Nitrogen adsorption–desorption isotherms were determined on samples that had been outgassed under vacuum for 12 h at 120 °C, using a Micromeritics ASAP 2020M instrument. The multiple-point Brunauer–Emmett–Teller (BET) method was used to calculate the SSA value of the materials. The SSA values of the clay minerals used in this study are showed in Table 1.

3. Results and discussion

3.1. Structures characterization

The d_{001}-value of Tlc at 0.95 nm (Fig. 2a) was equal to the individual layer thickness, indicating that the interlayer space was empty. On the other hand, the d_{001}-value for Mt was 1.48 nm because of the presence of hydrated (exchangeable) calcium ions in the interlayer space (Fig. 2a). The d_{001}-value of 1.88 nm for AlPMt corresponded to an interlayer separation (distance) of 0.92 nm. This value was close to the size of the Keggin-like $(Al_{13})^{7+}$ cation (0.9 nm), indicating the successful intercalation of Al_{13} into Mt (Plee et al., 1985). The d_{001}-value of AlPMt/500 at 1.78 nm was slightly smaller due to dehydroxylation of the cationic Al_{13} pillars after heating at 500 °C (Kloprogge et al., 1992, Kloprogge and Frost, 1999).

The basal spacing of the Z16-modified samples clearly depended on the clay mineral species used (Fig. 2b). In the case of montmorillonite, the d_{001}-value dramatically increased from 1.48 to 4.39 nm after modification with Z16, and a second order reflection appeared. This observation indicates successful penetration of Z16 into the interlayer space where the surfactant molecules adopted a variety of conformations (Zhu et al., 2012). On the other hand, the basal spacings of Z16-modified Tlc, AlPMt, and AlPMt/500 were comparable with those of the corresponding untreated (raw) clay mineral samples. Unlike that of montmorillonite, the

Table 1
The specific surface areas of clay minerals.

Samples	Specific surface area (m^2/g)
Tlc	19.9
Mt	69.5
AlPMt	283.2
AlPMt/500	261.5
Z16–AlPMt	17.9
Z16–AlPMt/500	13.4

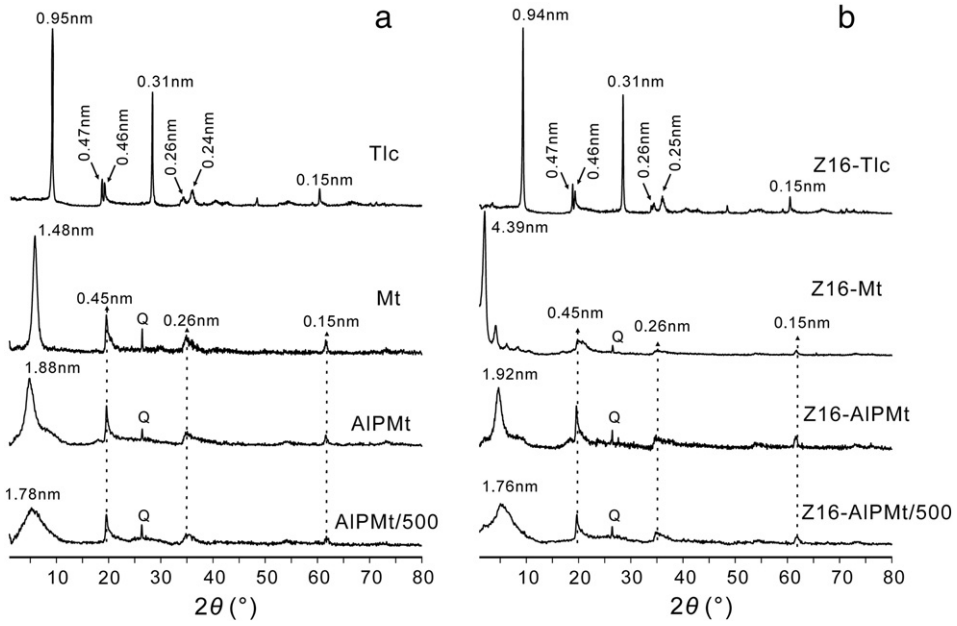

Fig. 2. X-ray diffraction (XRD) patterns of the original (raw) clay minerals (a), and the same samples after modification with Z16 (b). Q = quartz.

interlayer space of talc was inaccessible to Z16, while in the case of AlPMt and AlPMt/500, the surfactant molecules either failed to penetrate the interlayer spaces of AlPMt and AlPMt/500, or were loaded in the interlayer space of AlPMt in a configuration without causing interlayer expansion.

The SSA values of AlPMt (283.2 m^2/g) and AlPMt/500 (261.5 m^2/g) were much larger than that of Mt (69.5 m^2/g) (Table 1), which were consistent with the results of XRD. The type IV N_2 adsorption–desorption isotherms of AlPMt and AlPMt/500 were indicative of their microporosity (Fig. 3). The steep increase at low relative pressures corresponded to the filling of interpillar micropores in the interlayer space, and the hysteresis loop implied the interparticle mesopores space. After modification of Z16, however, SSA values of Z16–AlPMt and Z16–AlPMt/500 dramatically decreased to 17.9 and 13.4 m^2/g, respectively. The N_2 adsorption–desorption isotherms of Z16–AlPMt and Z16–AlPMt/500 showed that a much lower quantity of N_2 was adsorbed by these samples at low relative pressures than that adsorbed by AlPMt and AlPMt/500 (Fig. 3), indicating the dramatic decrease of micropores after loading of Z16. These findings

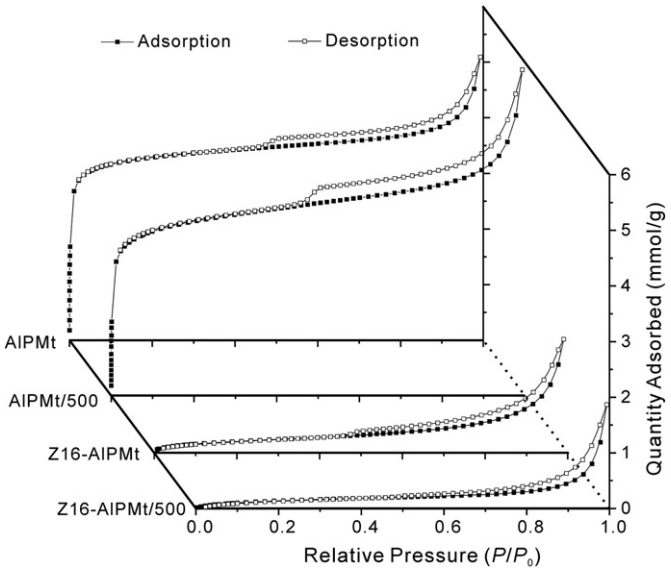

Fig. 3. N_2 adsorption–desorption isotherms of AlPMt and AlPMt/500, and their surfactant-modified products.

suggested that the interpillar micropores in interlayer space of AlPMt and AlPMt/500 were occupied by Z16 surfactant molecules; as a consequence, N_2 molecules could not be adsorbed into the interpillar spaces in the interlayer spaces of Z16–AlPMt and Z16–AlPMt/500.

3.2. Thermal analysis

The TG and DTG curves for the clay minerals were depicted in Fig. 4. In the DTG curve of Tlc (Fig. 3a), a single mass loss peak could be observed at ~928 °C, attributable to dehydroxylation of the layer structure. In the curve for Mt (Fig. 4b), on the other hand, two major peaks were obtained; the mass loss below 200 °C was due to the removal of water molecules associated with interparticle and interlayer surfaces, while that at 500–700 °C was ascribed to layer dehydroxylation. Like that of Mt, the DTG curve of AlPMt showed a large loss of mass at ~117 °C (Fig. 4c) from evaporation of adsorbed water, and a small loss in the range of 300 to 700 °C due to dehydroxylation of interlayer Al_{13} cations and the layer structure (Kloprogge and Frost, 1999; Occelli et al., 2000; Qin et al., 2010). The absence of a well-defined high-temperature peak indicates that dehydroxylation occurred gradually and at a uniform rate (Ma et al., 2014b). The high-temperature peak at ~622 °C in the curve of AlPMt/500 (Fig. 4d) was comparable to that shown by Mt (~635 °C), indicating that the pillared Al_{13} cations in AlPMt/500 had largely been dehydroxylated.

The TG and DTG curves of a freeze-dried solution of Z16 were illustrated in Fig. 5. The surfactant decomposed in the range of 250–350 °C, giving a distinct DTG peak at 306 °C. Since no peaks in the 200–500 °C range were detectable in the DTG curves of all four clay mineral samples (Tlc, Mt, AlPMt, AlPMt/500), peaks in the curves of the respective Z16-modified materials in this temperature range may be attributed to decomposition of the associated surfactant (Kooli, 2009; Zhu et al., 2012).

The TG and DTG curves for the Z16-modified clay mineral samples are depicted in Fig. 6. Z16–Tlc showed a major mass loss (5.95%) in the temperature range of 250–325 °C (Fig. 6a), corresponding to a DTG peak at ~294 °C (Fig. 6b). Since the position of this peak was close to that shown by freeze-dried pure Z16 (~306 °C; Fig. 5), the surfactant molecules were presumably adsorbed on external particle surfaces of Tlc via van der Waals forces.

Compared to that of raw Mt (Fig. 4b), the TG curve of Z16-modified Mt showed a marked decrease of mass loss at ~75 °C due to the adsorbed water (Fig. 6a). This observation may be explained in terms of the

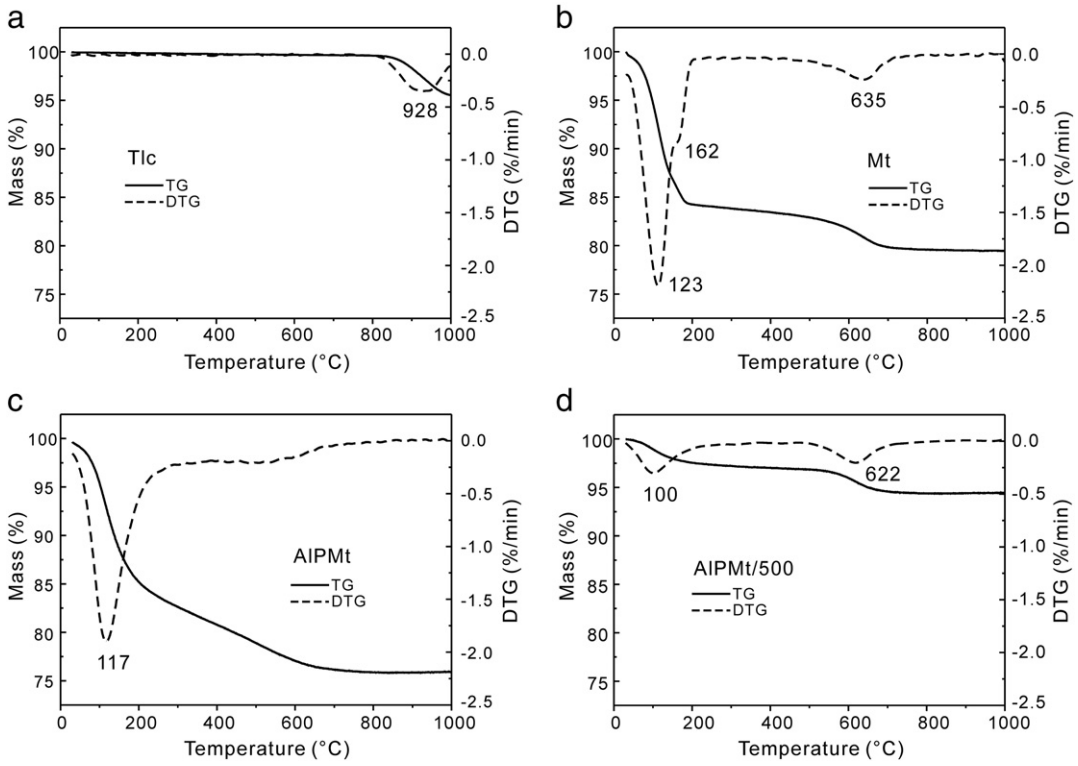

Fig. 4. Thermogravimetry (TG) and derivative thermogravimetry (DTG) curves of talc (Tlc), montmorillonite (Mt), Al_{13}-pillared montmorillonite (AlPMt), and calcined Al_{13}-pillared montmorillonite (AlPMt/500).

transformation of Mt from being hydrophilic to hydrophobic, following treatment with Z16 (Zhu et al., 2012). Further, the two main peaks at 336 and 404 °C in the DTG curve of Z16–Mt (Fig. 6b) occurred at a significantly higher temperature range than that of Z16 molecules associated with external particle surfaces of Tlc (294 °C). This finding suggests that intercalation into montmorillonite may protect Z16 molecules from thermal decomposition (Zhou et al., 2007; Zhu et al., 2011). In line with previous studies (He et al., 2005; Zhu et al., 2011, 2012), the mass loss at ~404 °C might be attributed to the decomposition of Z16, intercalated by cation exchange; while that at ~336 °C was due to the decomposition of surfactant molecules attached to the cationic counterparts by van der Waals forces, and electrostatic attraction between the quaternary ammonium and sulfonate groups of Z16 (Fig. 1). In addition, a small shoulder peak at ~300 °C could be observed, which is attributed to the decomposition of a small amount of Z16 molecules loaded in the particle pores with "house-of-cards" structure of Mt (He et al., 2005; Zhu et al., 2012).

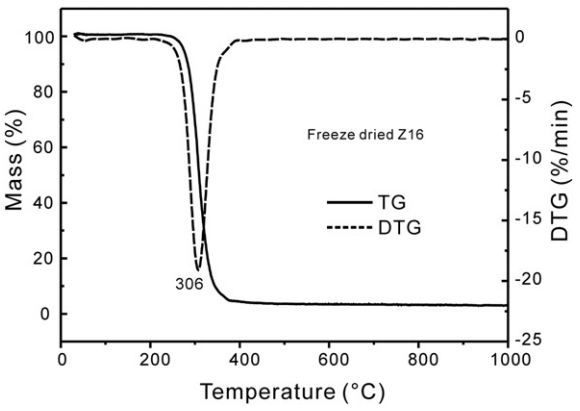

Fig. 5. TG and DTG curves of a freeze-dried solution of pure Z16.

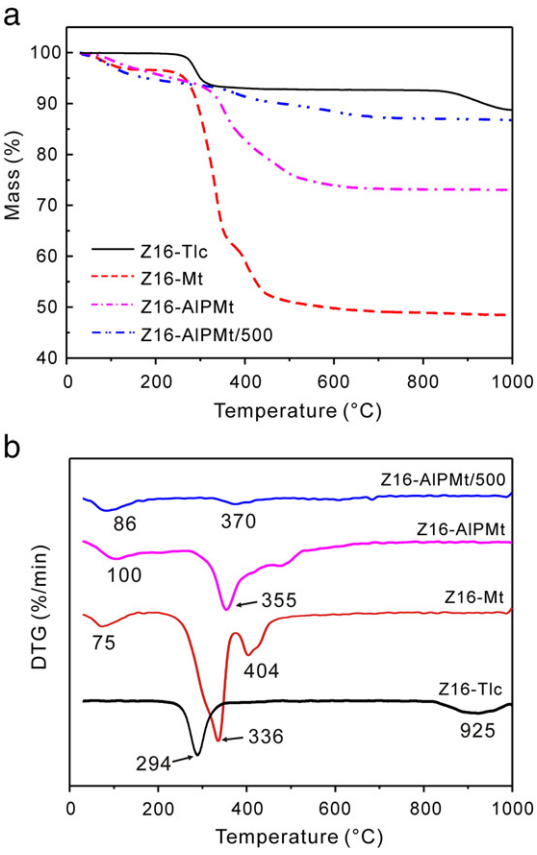

Fig. 6. TG (a) and DTG (b) curves of Z16-modified clay minerals.

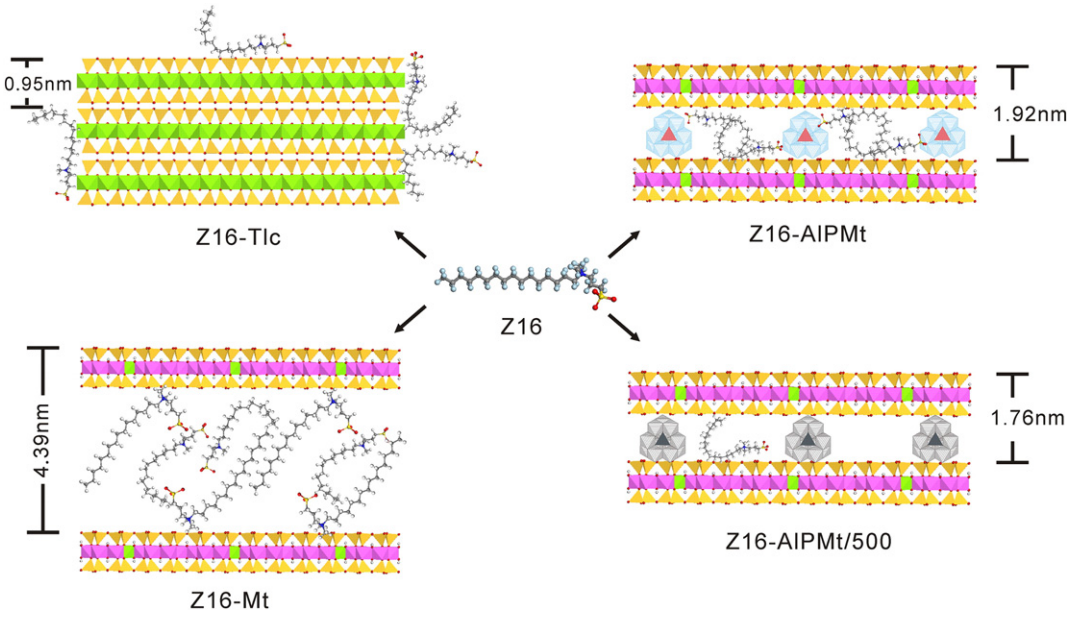

Fig. 7. A schematic diagram of different surfactant configurations in Z16-modified clay minerals.

In the case of Z16–AlPMt, the TG curve showed a mass loss of 17.27% in the temperature range of 300–500 °C (Fig. 6a) as compared with the value of 3.72% for the unmodified material (AlPMt). This observation was consistent with loading of Z16 molecules on AlPMt. The corresponding DTG peak at 355 °C for Z16-modified AlPMt (Fig. 6b) was indicative of surfactant molecules occupying the interlayer space (Fig. 7), which was consistent with the result of N_2 adsorption–desorption analysis. The mass loss between 300–500 °C for Z16–AlPMt/500 (3.8%) was slightly larger than that measured for the unmodified material (0.37%), but was significantly less than that shown by Z16–AlPMt in the same temperature range (Fig. 6a). This finding and the small DTG peak at ~370 °C (Fig. 6b) were indicative of limited uptake of Z16 into the interlayer space of AlPMt/500 (Fig. 7). Although the SSA and microporosity of AlPMt and AlPMt/500 were comparable, after Al_{13} cations were transformed into electrically neutral pillars via calcination, the capacity of AlPMt/500 for accommodating Z16 in its interpillar space was decreased. These findings and the thermal behavior of the Z16–AlPMt nanocomposite indicated that the adsorbed surfactant occupied the pore space between the interlayer $(Al_{13})^{7+}$ pillars to which they were held by electrostatic attraction involving the sulfonate groups.

4. Conclusions

The thermal behavior and stability of surfactants associated with clay minerals are known to be influenced by their bonding modes and location at the mineral surface. Here, X-ray diffraction (XRD) and thermogravimetry (TG) were used to assess the interactions of a zwitterionic surfactant, sulfobetaine (Z16), with talc (Tlc), montmorillonite (Mt), Al_{13}-pillared Mt (AlPMt), and AlPMt after calcination at 500 °C (AlPMt/500). XRD indicated that the interlayer space of Tlc was not accessible to Z16, confining adsorption to external particle surfaces. Accordingly, the surfactant decomposed at a very similar temperature to that of pure Z16.

In the case of Mt, however, more surfactants were intercalated, which caused a marked increase in basal spacing. Being thermally shielded, the interlayer Z16 decomposed at a higher temperature than that observed in the nanocomposite with Tlc. Intercalation of Z16 into Mt apparently occurred by cation exchange and intermolecular electrostatic attraction between the quaternary ammonium and sulfonate groups of the surfactant (Zhu et al., 2011). The basal spacing of AlPMt did not change noticeably after modification with Z16, but the SSA value and micropores dramatically decreased. Much less Z16 was taken up by AlPMt that had been calcined at 500 °C, although the SSA values of AlPMt and AlPMt/500 were very comparable. Calcination transformed Al_{13} cations to electrically neutral pillars (Occelli et al., 2000), decreasing the capacity of AlPMt/500 for accommodating Z16 in its interpillar space. These findings and the thermal behavior of the Z16–AlPMt nanocomposite, indicated that the adsorbed surfactant occupied the pore space between the interlayer $(Al_{13})^{7+}$ pillars to which they were held by electrostatic attraction involving the sulfonate groups (Ma et al., 2014b).

The interactions of organic surfactants with clay minerals have commonly been determined by a combination of adsorption, spectroscopic, and XRD measurements. This work has shown here that thermal analysis can provide a useful insight into the location and conformation of organic molecules at clay mineral surfaces.

Acknowledgments

We gratefully acknowledge financial support from the National Key Technology Research and Development Program of the Ministry of Science and Technology of China (Grant No. 2013BAC01B02), the Strategic Priority Research Program (Grant No. XDB05050200) of the Chinese Academy of Sciences, Team Project of Natural Science Foundation of Guangdong Province, China (Grant No. S2013030014241), and International Partnership Program for Creative Research Team (Grant No. 20140491534) of Chinese Academy of Science and State Administration of Foreign Experts Affairs. We thank the National Natural Science Foundation of China for the grants (Nos. 41272060, 41472044). We specially thank Benny K.G. Theng for his critical review of the manuscript. This is a contribution No. IS-2055 from GIGCAS.

References

Annabi-Bergaya, F., 2008. Layered clay minerals. Basic research and innovative composite applications. Microporous Mesoporous Mater. 107, 141–148.
Bergaya, F., Lagaly, G., 2001. Surface modification of clay minerals. Appl. Clay Sci. 19, 1–3.
Bergaya, F., Lagaly, G., 2013. General introduction: clays, clay minerals, and clay science. In: Bergaya, F., Lagaly, G. (Eds.), Handbook of Clay Science. Developments in Clay Science. Elsevier, pp. 1–19 (Chapter 1).
Bergaya, F., Jaber, M., Lambert, J.-F., 2011. Organophilic clay minerals. In: Galimberti, M. (Ed.), Rubber-clay Nanocomposites. John Wiley & Sons, Inc., pp. 45–86.

Bouberka, Z., Khenifi, A., Mahamed, H.A., Haddou, B., Belkaid, N., Bettahar, N., Derriche, Z., 2009. Adsorption of Supranol Yellow 4 GL from aqueous solution by surfactant-treated aluminum/chromium-intercalated bentonite. J. Hazard. Mater. 162, 378–385.
Chitrakar, R., Makita, Y., Sonoda, A., Hirotsu, T., 2011. Adsorption of trace levels of bromate from aqueous solution by organo-montmorillonite. Appl. Clay Sci. 51, 375–379.
Dentel, S.K., Jamrah, A.I., Sparks, D.L., 1998. Sorption and cosorption of 1,2,4-trichlorobenzene and tannic acid by organo-clays. Water Res. 32, 3689–3697.
Frost, R.L., Kristof, J., Horvath, E., 2009. Controlled rate thermal analysis of sepiolite. J. Therm. Anal. Calorim. 98, 423–428.
He, H.P., Ding, Z., Zhu, J.X., Yuan, P., Xi, Y.F., Yang, D., Frost, R.L., 2005. Thermal characterization of surfactant-modified montmorillonites. Clay Clay Miner. 53, 287–293.
He, H.P., Tao, Q., Zhu, J.X., Yuan, P., Shen, W., Yang, S.Q., 2013. Silylation of clay mineral surfaces. Appl. Clay Sci. 71, 15–20.
He, H.P., Ma, L.Y., Zhu, J.X., Frost, R.L., Theng, B.K.G., Bergaya, F., 2014. Synthesis of organoclays: a critical review and some unresolved issues. Appl. Clay Sci. 100, 22–28.
Heinz, H., Vaia, R.A., Krishnamoorti, R., Farmer, B.L., 2007. Self-assembly of alkylammonium chains on montmorillonite: effect of chain length, head group structure, and cation exchange capacity. Chem. Mater. 19, 59–68.
Kloprogge, J.T., Frost, R.L., 1999. Infrared emission spectroscopy of Al-pillared beidellite. Appl. Clay Sci. 15, 431–445.
Kloprogge, J.T., Geus, J.W., Jansen, J.B.H., Seykens, D., 1992. Thermal-stability of basic aluminum sulfate. Thermochim. Acta 209, 265–276.
Kooli, F., 2009. Thermal stability investigation of organo-acid-activated clays by TG–MS and in situ XRD techniques. Thermochim. Acta 486, 71–76.
Liu, H.M., Yuan, P., Liu, D., Tan, D.Y., He, H.P., Zhu, J.X., 2013. Effects of solid acidity of clay minerals on the thermal decomposition of 12-aminolauric acid. J. Therm. Anal. Calorim. 114, 125–130.
Ma, L.Y., Zhou, Q., Li, T., Tao, Q., Zhu, J.X., Yuan, P., Zhu, R.L., He, H.P., 2014a. Investigation of structure and thermal stability of surfactant-modified Al-pillared montmorillonite. J. Therm. Anal. Calorim. 115, 219–225.
Ma, L.Y., Zhu, J.X., He, H.P., Tao, Q., Zhu, R.L., Shen, W., Theng, B.K.G., 2014b. Al_{13}-pillared montmorillonite modified by cationic and zwitterionic surfactants: a comparative study. Appl. Clay Sci. 101, 327–334.
Occelli, M.L., Auroux, A., Ray, G.J., 2000. Physicochemical characterization of a Texas montmorillonite pillared with polyoxocations of aluminum II. NMR and microcalorimetry results. Microporous Mesoporous Mater. 39, 43–56.
Ouellet-Plamondon, C., Lynch, R.J., Al-Tabbaa, A., 2012. Comparison between granular pillared, organo- and inorgano–organo-bentonites for hydrocarbon and metal ion adsorption. Appl. Clay Sci. 67–68, 91–98.
Plee, D., Borg, F., Gatineau, L., Fripiat, J.J., 1985. High-resolution solid-state Al^{27} and Si^{29} nuclear magnetic-resonance study of pillared clays. J. Am. Chem. Soc. 107, 2362–2369.
Qi, L.Y., Fang, Y., Wang, Z.Y., Ma, N., Jiang, L.Y., Wang, Y.Y., 2008. Synthesis and physicochemical investigation of long alkylchain betaine zwitterionic surfactant. J. Surfactant Deterg. 11, 55–59.
Qin, Z.H., Yuan, P., Zhu, J.X., He, H.P., Liu, D., Yang, S.Q., 2010. Influences of thermal pretreatment temperature and solvent on the organosilane modification of Al_{13} intercalated/Al-pillared montmorillonite. Appl. Clay Sci. 50, 546–553.
Ray, S.S., Okamoto, M., 2003. Polymer/layered silicate nanocomposites: a review from preparation to processing. Prog. Polym. Sci. 28, 1539–1641.
Shen, Y.H., 2002. Removal of phenol from water by adsorption–flocculation using organobentonite. Water Res. 36, 1107–1114.
Tahani, A., Karroua, M., El Farissi, M., Levitz, P., van Damme, H., Bergaya, F., Margulies, L., 1999. Adsorption of phenol and its chlorine derivatives on PILCS and organo-PILCS. J. Chim. Phys. 96, 464–469.
Theng, B.K.G., 2012. Formation and Properties of Clay–Polymer Complexes. second ed. Elsevier B.V, Amsterdam.
Theng, B.K.G., Churchman, G.J., Gates, W.P., Yuan, G., 2008. Organically modified clays for pollutant uptake and environmental protection. In: Huang, Q., Huang, P.M., Violante, A. (Eds.), Soil Mineral—Microbe–Organic Interactions: Theories and Applications. Springer-Verlag, Berlin, pp. 145–174.
Xi, Y., Martens, W., He, H., Frost, R.L., 2005. Thermogravimetric analysis of organoclays intercalated with the surfactant octadecyltrimethylammonium bromide. J. Therm. Anal. Calorim. 81, 91–97.
Xi, Y.F., Zhou, Q., Frost, R.L., He, H.P., 2007. Thermal stability of octadecyltrimethylammonium bromide modified montmorillonite organoclay. J. Colloid Interface Sci. 311, 347–353.
Xie, W., Xie, R.C., Pan, W.P., Hunter, D., Koene, B., Tan, L.S., Vaia, R., 2002. Thermal stability of quaternary phosphonium modified montmorillonites. Chem. Mater. 14, 4837–4845.
Zhou, Q., Frost, R.L., He, H.P., Xi, Y.F., 2007. Changes in the surfaces of adsorbed p-nitrophenol on methyltrioctadecylammonium bromide organoclay — an XRD, TG, and infrared spectroscopic study. J. Colloid Interface Sci. 314, 405–414.
Zhu, L.Z., Chen, B.L., 2000. Sorption behavior of p-nitrophenol on the interface between anion–cation organobentonite and water. Environ. Sci. Technol. 34, 2997–3002.
Zhu, L.Z., Zhu, R.L., 2007. Simultaneous sorption of organic compounds and phosphate to inorganic–organic bentonites from water. Sep. Purif. Technol. 54, 71–76.
Zhu, L.Z., Chen, B.L., Shen, X.Y., 2000. Sorption of phenol, p-nitrophenol, and aniline to dual-cation organobentonites from water. Environ. Sci. Technol. 34, 468–475.
Zhu, R., Wang, T., Ge, F., Chen, W., You, Z., 2009a. Intercalation of both CTMAB and Al_{13} into montmorillonite. J. Colloid Interface Sci. 335, 77–83.
Zhu, R.L., Zhu, L.Z., Zhu, J.X., Ge, F., Wang, T., 2009b. Sorption of naphthalene and phosphate to the CTMAB-Al_{13} intercalated bentonites. J. Hazard. Mater. 168, 1590–1594.
Zhu, J.X., Qing, Y.H., Wang, T., Zhu, R.L., Wei, J.M., Tao, Q., Yuan, P., He, H.P., 2011. Preparation and characterization of zwitterionic surfactant-modified montmorillonites. J. Colloid Interface Sci. 360, 386–392.
Zhu, J.X., Shen, W., Ma, Y.H., Ma, L.Y., Zhou, Q., Yuan, P., Liu, D., He, H.P., 2012. The influence of alkyl chain length on surfactant distribution within organo-montmorillonites and their thermal stability. J. Therm. Anal. Calorim. 109, 301–309.